

In situ estimation of fatigue crack parameters by digital image correlation under cyclic loading with single overload

A V Eremin¹, A V Byakov¹, P S Lyubutin¹, S V Panin^{1,2} and V V Titkov¹

¹Institute of Strength Physics and Materials Science, Tomsk, Russia

²National Research Tomsk Polytechnic University, Tomsk, Russia

ave@ispms.tsc.ru

Abstract. The paper represents the investigation of crack propagation in aluminium alloy AA2024 in a case of constant cyclic loading with single overload. The parameters of the process were evaluated by means of optical and noncontact digital image correlation technique which allows precise in situ measurements and provides local strain data. There have been analysed strain fields, local strains at the crack tip and crack closure level in order to reveal the effect of overload on crack growth parameters. Results are consistent with published data and developed mathematical models – the highest impact is emerged when crack extended into overload plastic zone by 30%.

1. Introduction

Numerous structures and components are subjected to cyclic loading. Fatigue is the reason for the most of the fractures and accidents in engineering, however huge amount of experimental research and theoretical modelling cover mostly constant amplitude case while the real components undergo random spectrum loading. Such non-uniform loading attracts much interest for prognosis of residual life time and detailed behaviour of the crack. Most researchers utilize conventional technique for studying crack growth parameters via crack opening displacement gauge (COD) which is mounted at the edge of the specimen according to the standard ASTM E647 “Standard Test Method for Measurement of Fatigue Crack Growth Rates”. This technique is based on the compliance principle which leads to low sensitivity and thus requires several loading-unloading cycle for more precise measurements of closure level and crack length. Such drawbacks limit the application of the gauge for evaluation of dynamic processes, particularly spectrum loading where the each next cycle overlap the effect of the previous one. According to the described aspects the COD gauge require complicated procedure for precise evaluation of loading history effects [1,2].

The other widely used method is optical or scanning electron microscopy which provides the most accurate results, but they might be obtained only after fracture, not during the test. Therefore it is not possible to perform detailed study of the crack parameters evolution which is critical in a case of random non-uniform loading fatigue tests.

The new approach which has prospects to replace the COD is digital image correlation technique, which allow one to determine the displacement and strain fields on the specimen surface. By post-processing of these data it is possible to evaluate the required characteristics of crack propagation process. The fundamental capabilities of the DIC was founded by M. Sutton [3,4].



The successive results for evaluation of crack-tip fields are published in [5,6]. Such technique was successfully implemented for crack growth characterization [7] including in presence of overload [8].

The current study is continuation of DIC enhancement for fatigue crack characterization and its implementation for different materials and loading conditions. The purpose of the work is measurements of crack growth parameters (propagation rate, strains at the tip and crack closure) in aluminium alloy AA 2024 under single overload by means of digital image correlation.

2. Laboratory equipment and evaluation of crack parameters

The fatigue tests were performed using servo-hydraulic testing machine BISS Nano 15 kN. As was mentioned above higher sensitivity of measurements of crack parameters in comparison with conventional COD method could be achieved with optical measurements at high magnification. Such a technique was implemented in present study by using optical microscope equipped with c-mount CCD camera Basler piA2400-17gc. The observed region was $\sim 2.5 \times 2.0$ mm that provides the image scale of $1.04 \mu\text{m}/\text{px}$. But such technique has difficulties for automatization due to crack growth out of the observed region. Thus the set up contains high-precise linear actuators with step motors for smooth microscope motion in X, Y and Z directions.

In this study several major crack growth parameters have been evaluated by means of digital image correlation technique by post-processing of displacement/strain fields.

2.1. Strains at the crack tip

The crack length and coordinates of the crack tip were obtained manually directly from acquired microscopic images and on this basis crack growth rate (CGR) was evaluated. In order to evaluate the mechanical response of the materials to the applied load the program extensometer tool was used. This extensometer locates at the crack tip and provides strain values based on the displacements obtained via DIC (see figure 1) and in doing this way local strains were evaluated.

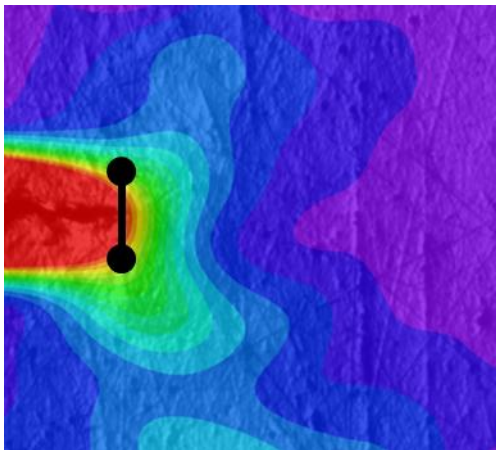


Figure 1. Position of the program extensometer on the ϵ_{yy} (y axis is vertical) strain field at the crack tip.

2.2. Hysteresis loops

As far as the surface images were acquired during the whole loading cycle, thus it is possible to evaluate the characteristic of deformation processes in the vicinity of the crack tip in the form of hysteresis loop presented in figure 2.

The shape of the loop characterizes nonlinear behaviour of the material at the crack tip due to local plastic deformations and crack closure – the wider ascending and descending parts, the higher level of plastic deformations. The plasticity could be numerically characterized by interior loop area which has a meaning of plastic deformation energy, while crack closure requires more complicated evaluation technique described in the next subsection.

2.3. Effective loading ratio

The value of effective loading ratio numerically describes the crack closure process. The computation procedure contains the following steps (illustrated in figure 2):

- calculation of the total loop area S ;
- evaluation of loading value P_{mean} which cut the loop on two equal parts ($S_1=S_2$);
- in a case of no crack closure the loop will be symmetric and the relation

$$P_{max} - P_{mean} = P_{mean} - P_{min}$$

will be efficient, while in presence of closure $P_{max} - 2\Delta P = P_{closure} > P_{min}$ and therefore the effective loading ratio could be found from the following equation:

$$R_{eff} = 2 \frac{P_{mean}}{P_{max}} - 1$$

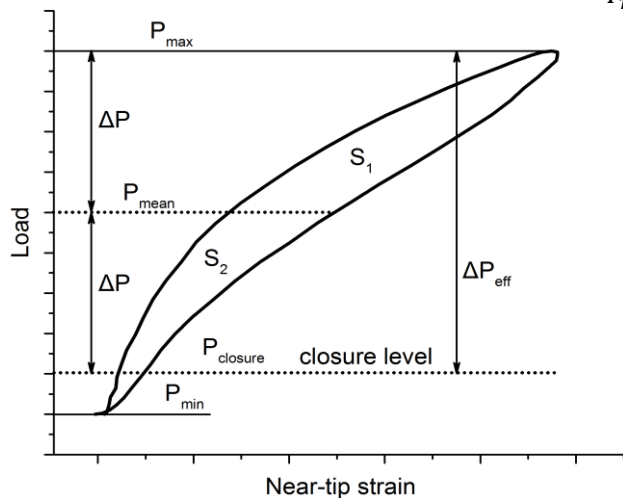


Figure 2. Mechanical response of the material in the vicinity of the crack tip to the applied loading.

3. Schematic of cyclic loading with single overload

The fatigue tests were performed for the notched specimen cut from 3 mm aluminium plate. The schematic of the loading procedure is presented in figure 3 and consists of measurement cycle before overload, overload cycle and cycles after overload at different intervals.

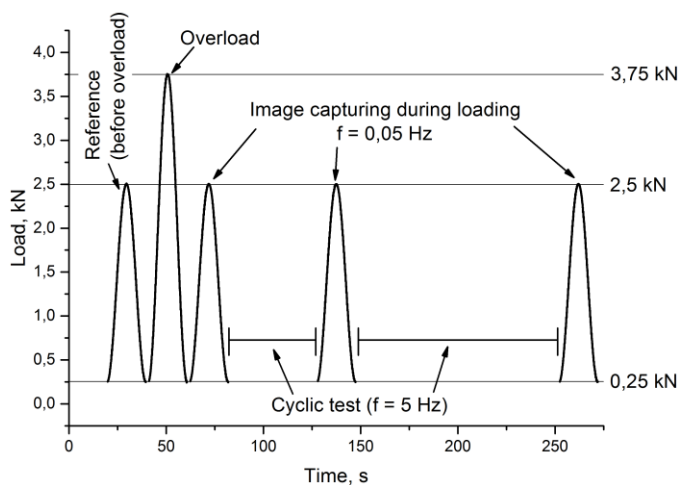


Figure 3. Schematic of the fatigue loading procedure with single overload (50% of nominal load). It consists of basic cycles (0.25-2.5 kN) – some of them had reduced cyclic frequency during which image acquisition has been performed and single overload (0.25-3.75 kN).

According to linear-elastic fracture mechanics the stress intensity factors at the beginning of the fatigue tests were the following: $K_{max}=12.9 \text{ MPa}\cdot\sqrt{\text{m}}$, while $K_{OvL}=19.3 \text{ MPa}\cdot\sqrt{\text{m}}$ that corresponds to the plastic zone size for plane stress state is $R_{OvL}=580 \text{ }\mu\text{m}$. Nominal load level provides the plastic zone

ahead of the crack tip from 295 μm at the beginning of the test to 350 μm at the end whilst the crack extended from ~ 15.5 to ~ 16.6 mm.

4. Experimental results and discussion

The graph in figure 4 illustrates the changes of CGR due to single overload. At the beginning of the test the average growth rate was ~ 0.01 $\mu\text{m}/\text{cycle}$. Single overload cycle results in crack extension for 35 μm , but it could be attributed to better visualisation of the crack tip due to blunting rather than real propagation. Crack tip blunting and residual compressive stresses after overload retarded the crack growth for first several cycles, but there were removed very fast, because after 10 cycles the rate was 0.6 $\mu\text{m}/\text{cycle}$. The subsequent crack tip re-sharpness and extension in the overload plastic zone leads to the pronounced retardation of the growth rate to 0.004 $\mu\text{m}/\text{cycle}$ at 30% of R_{OVL} . 30% is the critical value where the effect of overload is a maximum; further propagation leads to accelerated CGR up to 0.05 $\mu\text{m}/\text{cycle}$ when crack tip completely exits the overload plastic zone.

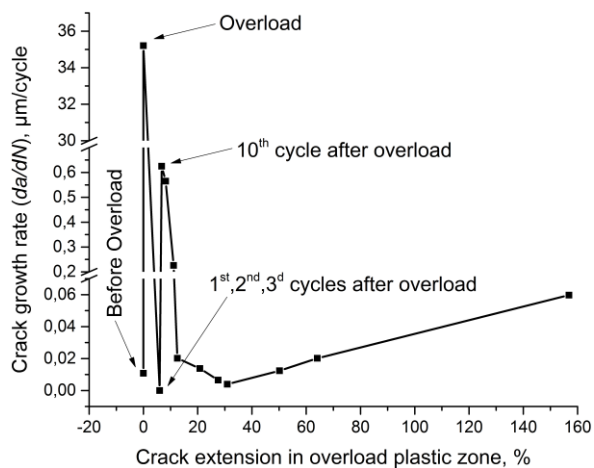


Figure 4. Crack growth rate before and after overload depending on the crack extension in the overload plastic zone.

Figure 5 shows the evolution of maximum strain value measured at the crack tip by program extensometer. Before the overload maximum strain was $4.7 \cdot 10^{-3}$, then overload increased ε_{max} to $13 \cdot 10^{-3}$ which means that crack tip was blunted due to intensive plastic flow. After overload crack tip re-sharpening occurred rather fast – after 500-1000 nominal cycles it recovers to the original values, but the sharp tip in presence of residual stresses caused by plastic deformations leads to development of crack closure and thus ε_{max} continue to reduce. When the crack extended to the overload plastic zone by 20-30% the strains at the tip start increasing.

Very important characteristic of fatigue crack propagation process is closure level, named in the manuscript efficient loading ratio. The changing of R_{eff} is shown in figure 6. Fatigue tests were performed at the ratio of 0.1, however at the beginning of the fatigue test the closure was existed and the efficient ratio was slightly higher – $R_{eff}=0.12$. Higher ratio means that real stress range at the tip is reduced. Overload results in crack blunting which keeps the tip opened, but re-sharpening process occurring over the several cycles restores positive values. When the crack tip reaches 20% of overload plastic zone the closure level rises very fast to its highest value and leads to significant crack retardation. Recovering of closure level ends at 50-60% of the overload plastic zone size and remains constant; however the final value is slightly higher than the initial one.

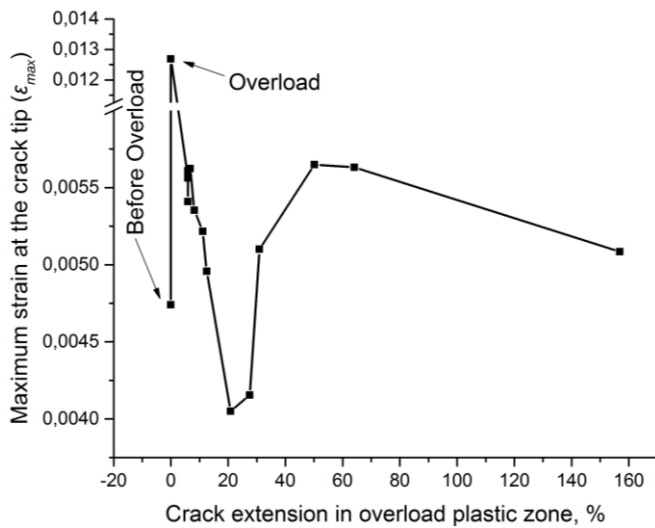


Figure 5. Maximum strain (ϵ_{max}) at the crack tip for measurements cycles before and after overload depending on the crack extension in the overload plastic zone.

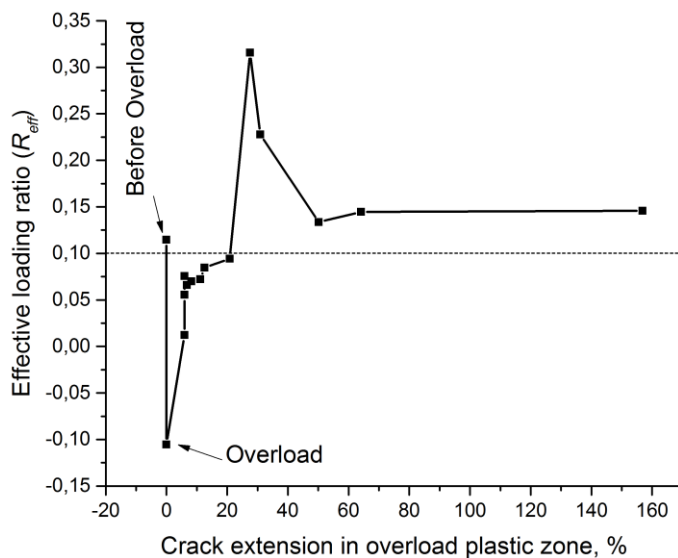


Figure 6. Effective loading ratio (R_{eff}) at measurements cycles before and after overload depending on the crack extension in the overload plastic zone.

5. Conclusion

The study demonstrates the procedure for evaluation and changes of crack growth parameters (crack growth rate da/dN , maximum strain at the crack tip ϵ_{max} and effective loading ratio R_{eff}) evaluated by means of post-processing of strain fields obtained via digital image correlation technique. It is seen that proposed technique is sensitive to the local changes in strains and closure levels.

The fatigue test of AA2024 specimens demonstrates that after overload there occur several processes – crack tip blunting which remains at the first few cycles and crack re-sharpening which accelerates crack growth rate and increasing of closure level due to influence of plastically deformed area around the crack tip. Blunting was removed after several cycles and leads to increase of closure level. In order to be increased and play a significant role the latter needs extension into the overload plastic region where residual compressive stresses will keep the tip partially closed and thereby reduces stress concentration level. Thus when the crack tip extended into the overload plastic zone at 30% it leads to minimum of crack growth rate ($da/dN=0.004 \mu\text{m}/\text{cycle}$) and strains at the crack tip

($\epsilon_{max}=4 \cdot 10^{-3}$) while loading ratio reaches its maximum ($R_{eff}=0.32$, when initial ratio was $R=0.1$). When crack achieves 60% of overload plastic zone the influence of overload is almost removed and the parameters return to the values close to the initial.

Acknowledgements

The work was partially supported by RF President Council Grants for the support of young researchers № MK-6762.2018.9 and by RFBR 18-38-00659 mol_a.

References

- [1] Salvati E, Zhang H, Fong K S, Song X and Korsunsky A M 2017 Separating plasticity-induced closure and residual stress contributions to fatigue crack retardation following an overload *J. Mech. Phys. Solids* **98** 222–35
- [2] Newman J C, Walker K F and Liao M 2015 Fatigue crack growth in 7249-T76511 aluminium alloy under constant-amplitude and spectrum loading *Fatigue Fract. Eng. Mater. Struct.* **38** 528–39
- [3] Sutton M A, McNeill S R, Helm J D and Chao Y J Advances in Two-Dimensional and Three-Dimensional Computer Vision *Photomechanics* (Berlin, Heidelberg: Springer Berlin Heidelberg) pp 323–72
- [4] Sutton M A, Matta F, Rizos D, Ghorbani R, Rajan S, Mollenhauer D H, Schreier H W and Lasprilla A O 2017 Recent Progress in Digital Image Correlation: Background and Developments since the 2013 W M Murray Lecture *Exp. Mech.* **57** 1–30
- [5] Carroll J D, Abuzaid W, Lambros J and Sehitoglu H 2013 High resolution digital image correlation measurements of strain accumulation in fatigue crack growth *Int. J. Fatigue* **57** 140–50
- [6] Lopez-Crespo P, Moreno B, Lopez-Moreno A and Zapatero J 2015 Characterisation of crack-tip fields in biaxial fatigue based on high-magnification image correlation and electro-spray technique *Int. J. Fatigue* **71** 17–25
- [7] Sgambitterra E, Maletta C, Furgiuele F and Sehitoglu H 2018 Fatigue crack propagation in [0 1 2] NiTi single crystal alloy *Int. J. Fatigue* **112** 9–20
- [8] Wang D Q, Zhu M L, Xuan F Z and Tong J 2017 Crack tip strain evolution and crack closure during overload of a growing fatigue crack *Frat. ed Integrita Strutt.* **11** 143–8